RESEARCH ARTICLE

Key Points:
- The simulations using CLM4.5 driven by reanalysis-based forcing data sets reasonably reproduce the observed long-term temporal variations in the timing and duration of the near-surface soil freeze
- The CRUNCEP-based simulation is overall superior to the CFSR-, ERA-I-, and MERRA-based simulations
- The variation in the atmospheric forcing data set produces a shortening in simulated annual near-surface soil freeze duration with a range of 6.94 to 8.77 days from 1979 to 2009

Simulation of Changes in the Near-Surface Soil Freeze/Thaw Cycle Using CLM4.5 With Four Atmospheric Forcing Data Sets

Donglin Guo[1,2,3] (iD), **Aihui Wang**[1] (iD), **Duo Li**[4], and **Wei Hua**[2]

[1]Nansen-Zhu International Research Centre, Institute of Atmospheric Physics, Chinese Academy of Sciences, Beijing, China, [2]Joint Laboratory for Climate and Environmental Change, Chengdu University of Information Technology, Chengdu, China, [3]Key Laboratory of Meteorological Disaster, Ministry of Education/Collaborative Innovation Center on Forecast and Evaluation of Meteorological Disasters, Nanjing University of Information Science and Technology, Nanjing, China, [4]National Climate Center, Beijing, China

Abstract Change in the near-surface soil freeze/thaw cycle is critical for assessments of hydrological activity, ecosystems, and climate change. Previous studies investigated the near-surface soil freeze/thaw cycle change mostly based on in situ observations and satellite monitoring. Here numerical simulation method is tested to estimate the long-term change in the near-surface soil freeze/thaw cycle in response to recent climate warming for its application to predictions. Four simulations are performed at $0.5° \times 0.5°$ resolution from 1979 to 2009 using the Community Land Model version 4.5, each driven by one of the four atmospheric forcing data sets (i.e., one default Climate Research Unit-National Centers for Environmental Prediction [CRUNCEP] and three newly developed Modern Era Retrospective-Analysis for Research and Applications, Climate Forecast System Reanalysis, and European Centre for Medium-Range Weather Forecasts Reanalysis Interim). The observations from 299 weather stations in both Russia and China are employed to validate the simulated results. The results show that all simulations reasonably reproduce the observed variations in the ground temperature, the freeze start and end dates, and the freeze duration (the correlation coefficients range from 0.47 to 0.99, and the Nash-Sutcliffe efficiencies range from 0.19 to 0.98). Part of the simulations also exactly simulate the trends of the ground temperature, the freeze start and end dates, and the freeze duration. Of the four simulations, the results from the simulation using the CRUNCEP data set show the best overall agreement with the in situ observations, indicating that the CRUNCEP data set could be preferentially considered as the basic atmospheric forcing data set for future prediction. The simulated area-averaged annual freeze duration shortened by 8.03 days on average from 1979 to 2009, with an uncertainty (one standard deviation) of 0.67 days caused by the different atmospheric forcing data sets. These results address the performance of numerical model in simulating the long-term changes in the near-surface soil freeze/thaw cycle and the role of different atmospheric forcing data sets in the simulation, which are useful for the prediction of future freeze/thaw dynamics.

1. Introduction

Each year, approximately 50% of the Northern Hemisphere land area undergoes a seasonal transition from predominantly frozen conditions to thawed conditions (Kim et al., 2011). At high northern latitudes, the near-surface soil freeze/thaw cycle is closely linked to the surface energy budget (Guo et al., 2011a, 2011b), hydrological activity (Rawlins et al., 2005; Wang et al., 2009; Yang et al., 2014), vegetation growing season length and productivity (Kimball et al., 2004, 2006), land-atmosphere CO_2 exchange (Kurganova et al., 2007; Picard et al., 2005), and global weather patterns (Chen et al., 2014; Li & Chen, 2013; Qin et al., 2014; Randerson et al., 1999; Wang et al., 2003). The near-surface soil freeze/thaw cycle is sensitive to climate change (Kim et al., 2012). Recent global warming has resulted in significant changes in the timing and duration of near-surface soil freezing (Guo & Wang, 2014; Kim et al., 2012; Wang et al., 2015). In turn, such changes largely affect the hydrological processes, terrestrial ecosystems, and global climate (Cheng & Wu, 2007; Kim et al., 2012; Qin et al., 2014; Yang et al., 2010; Yi et al., 2011). These impacts require an accurate estimate of the changes in the near-surface soil freeze/thaw cycle, which is a prerequisite for evaluating the impacts.

In situ observations have widely been used to uncover changes in the near-surface soil freeze/thaw cycle (Anandhi et al., 2013; Henry, 2008; Menzel et al., 2003; Peng et al., 2016; Sinha & Cherkauer, 2008; Wang et al., 2015; Zhao et al., 2004). Based on observations from 41 weather stations, Menzel et al. (2003)

reported that the freeze-free period in Germany was extended by 0.11–0.49 days year^{-1} from 1951 to 2000. Using the observations from 31 sites in Canada, Henry (2008) found that annual number of days of soil freezing declined from 1966 to 2004 as a result of the increase in the mean winter air temperature. Anandhi et al. (2013) analyzed the frost indices at 23 weather stations in Kansas, USA, and found that the last spring freeze occurred earlier and the first fall freeze occurred later at most stations over their study period. More recently, using the data from 636 weather stations in China, Wang et al. (2015) found that the freeze duration shortened at a rate of 0.25 ± 0.04 days year^{-1} from 1956 to 2006 as a result of a delayed freeze start date, at a rate of 0.10 ± 0.03 days year^{-1}, and earlier freeze end date, at a rate of −0.15 ± 0.02 days year^{-1}. These observation-based studies report important regional facts of changes in the near-surface freeze/thaw cycle but are limited for providing independent information on the global scales as a result of the sparse distribution of global weather station networks, especially at high latitudes and high elevations.

The satellite remote sensing technique can overcome this limitation of observation-based studies and is well suited for the monitoring of the global near-surface soil freeze/thaw status (Kim et al., 2011, 2012; McDonald et al., 2004; Smith et al., 2004; Zhang & Armstrong, 2001; Zhang et al., 2003). Using the evidence from microwave remote sensing, McDonald et al. (2004) reported that the spring thaw advanced by approximately 8 days from 1988 to 2001 in the pan-Arctic basin and Alaska. Smith et al. (2004) developed a satellite database technique to identify the timing of the freeze/thaw transitions in the high northern latitude area from 1988 to 2002 and detected earlier spring thaw dates in the tundra and larch biomes in Eurasia and later autumn freeze dates in the evergreen conifer forests in North America. An advancing spring thaw trend (0.7 days year^{-1}) and a delaying autumn freeze trend (0.5 days year^{-1}) were also identified on the Tibetan Plateau by Li et al. (2012) using the Special Sensor Microwave/Imager data. More recently, Kim et al. (2011) and Kim et al. (2012) developed a global product of the daily landscape freeze/thaw status based on the passive microwave remote sensing record and found that the annual nonfrozen season increased by 0.19 days year^{-1} on average from 1979 to 2008 over the Northern Hemisphere as a whole.

Proper simulation of the change in the near-surface soil freeze/thaw cycle is essential for accurately predicting these changes under a warming climate scenario. Previous simulation studies mainly concentrated on model improvements for more accurate simulation of the soil freeze/thaw cycle over one or several years (Rawlins et al., 2013; Schaefer et al., 2009; Slater et al., 1998; Yi et al., 2006). The improvements include, for example, modification of the hydraulic conductivity parameterization (Slater et al., 1998), update of the snow model (Rawlins et al., 2013), representation of the thermal and hydraulic properties of the soil organic matter (Schaefer et al., 2009), and deepening of the soil column in the land surface model (Schaefer et al., 2009). These improvements have significantly advanced model performances of the simulations of the soil annual freezing and thawing processes. However, how do long-term temporal changes in the near-surface soil freeze/thaw cycle in the Northern Hemisphere be estimated by numerical models? And to what extent do the variations in the atmospheric forcing data set affect the estimation of the soil freeze/thaw cycle change? These questions are closely related to the prediction of future dynamics in the freeze/thaw cycle, but they have not been well understood.

The objectives of this study are as follows: (1) use the long-term temporal in situ observations to assess the performance of the numerical model in estimating the changes of the near-surface soil freeze/thaw cycle in the Northern Hemisphere and (2) examine the impacts of different atmospheric forcing data sets on the simulation of the near-surface soil freeze/thaw cycle. The latest version of the Community Land Model version 4.5 (CLM4.5) was employed in this study. In addition, four atmospheric forcing data sets (one is the default data set and three others are newly developed data sets) were used for assessing the uncertainties in the simulated results caused by the atmospheric inputs.

2. Data, Model, Experimental Design, and Methods

2.1. Data

Four atmospheric forcing data sets are used for driving the land surface model, including the Climate Research Unit-National Centers for Environmental Prediction (CRUNCEP) (Viovy, 2011), the National Oceanic and Atmospheric Administration Climate Forecast System Reanalysis (CFSR) (Wang et al., 2016), the European Centre for Medium-Range Weather Forecasts Reanalysis Interim (ERA-I) (Wang et al., 2016), and the National Aeronautics and Space Administration Modern Era Retrospective-Analysis for Research

Table 1

Horizontal Resolution of the Four Atmospheric Forcing Data Sets, the Climatology, and the Trend in the Surface Air Temperature and Ground Temperature From the Simulations Based on the Four Atmospheric Forcing Data Sets

Forcing data set	Resolution (°lon × °lat)	Mean annual surface air temperature (°C)		Mean annual ground temperature (°C)	
		Climatology (1981–2000)	Trend (per decade, 1979–2009)	Climatology (1981–2000)	Trend (per decade, 1979–2009)
CFSR	0.5° × 0.5°	−2.09	0.44	−4.86	0.42
ERA-Interim	0.5° × 0.5°	−2.06	0.42	−4.44	0.42
MERRA	0.5° × 0.5°	−1.96	0.42	−3.78	0.42
CRUNCEP	0.5° × 0.5°	−2.82	0.40	−5.16	0.43

Note. All variables are mean values that are averaged in the simulated present-day (1981–2000) regions of permafrost and seasonally frozen ground shown in Figure 1.

and Applications (MERRA) (Wang et al., 2016) (Table 1). CRUNCEP is a new default data set of the CLM, which was developed by combining the Climate Research Unit TS3.2 monthly observations (resolution: 0.5° × 0.5°) (Mitchell & Jones, 2005; Sun, 2017) and the National Centers for Environmental Prediction six-hourly reanalysis data (resolution: 2.5° × 2.5°) (Fan et al., 2016; Gao, 2017; Kalnay et al., 1996). The data cover a period of 1901–2010 at a spatial (temporal) resolution of 0.5° × 0.5° (six-hourly). The CRUNCEP data have been employed to force CLM for studies on various topics such as vegetation growth, evapotranspiration, permafrost dynamics (Guo & Wang, 2017; Mao et al., 2013; Shi et al., 2013).

The CFSR, ERA-I, and MERRA forcing data sets were developed based on the reanalysis data of CFSR (Saha et al., 2010), ERA-I (Chen et al., 2017; Dee et al., 2011), and MERRA (Rienecker et al., 2011), respectively. They have a common period of 1979 to the present and resolution of 0.5° × 0.5° but have different temporal resolutions at six-hourly (CFSR), three-hourly (ERA-I), and hourly (MERRA). A bilinear interpolation method was employed to yield the air temperature, air pressure, wind speed, specific humidity, and downward shortwave radiation in the three forcing data sets. A new downscaling method was used to calculate the precipitation to ensure that the precipitation amount in a specified area remains the same before and after downscaling. Details for the development of these three data sets can be found in Wang et al. (2016). Observation-based evaluations showed that the model simulations based on these three forcing data sets performed reasonably for predicting the soil temperature, soil moisture, runoff, snow, and surface heat fluxes (Guo et al., 2017; Wang et al., 2016).

The ground temperature observations used to validate the simulated results are derived from the meteorological stations located in the frozen ground regions in Russia (RGT) and China (CGT). The RGT data cover the period of 1966–2015, and the data from 112 stations selected from total 495 stations are used in this study for the model validation because these stations have long-term continuous data for the ground temperature, from which the freeze start and end dates can be calculated (Figure 1). The temporal resolution of the original RGT data is three-hourly, which is averaged to daily to identify the soil freeze/thaw status. A strict quality control procedure was conducted in the postprocessing stage for RGT data, which ensures that the data are reliable. These data and more detailed descriptions can be obtained from http://meteo.ru/english/data/.

The daily CGT data are derived from the Data and Information Center, China Meteorological Administration. The data that we obtained cover the total period of 1951–2008 but are not continuous at many stations. The data at 187 stations are used for validation of the model in this study, and their locations can be seen in Figure 1. The CGT data have been checked with a basic logic test and a spatial consistency test for data quality control. These data are reliable and have been previously used to research the changes in the near-surface soil freeze/thaw cycle in China (e.g., Wang et al., 2015). Both the RGT and CGT data are measured on the bare soil surface or snow cover surface. To evaluate the performance of model, the station observations first were averaged across stations as the regional mean and then they were compared to the simulated results averaged across the corresponding simulation grids.

2.2. Model

The latest version of CLM, CLM4.5 (Oleson et al., 2013), was used in this study, which is an updated version of CLM4.0. A series of important modifications have been incorporated within CLM since version 3.0 (Lawrence et al., 2011). These modifications are related to the snow model (Flanner et al., 2007; Wang & Zeng, 2009),
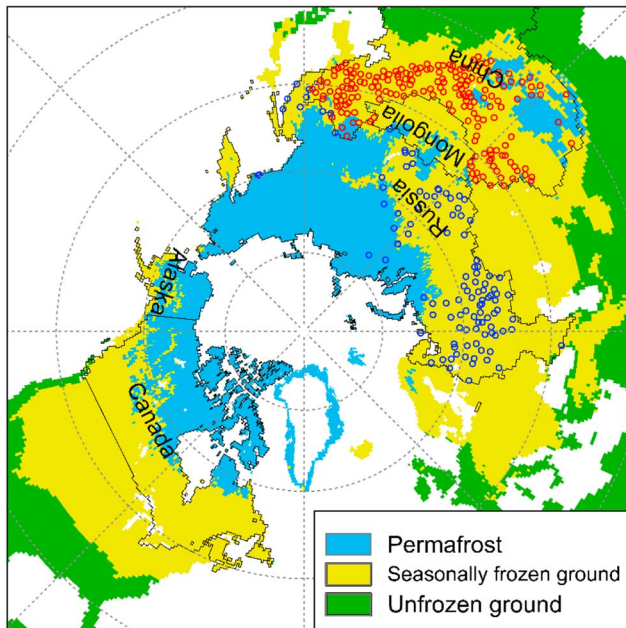
Figure 1. Distribution of the weather stations used to validate the model. The extents of the different ground states, which create the base map, are derived from CLM4.5 and driven by the default CRUNCEP forcing dataset. The blue (red) circles represent the weather stations in Russia (China).

carbon-nitrogen biogeochemical model (Thornton et al., 2009; Xie et al., 2016), land surface types data set (Lawrence & Chase, 2007), urban model (Oleson et al., 2008), transient land cover and land use change (Lawrence & Chase, 2010), and soil model (Lawrence et al., 2012). The improvements relevant to the frozen ground consist of an explicit description of soil freezing and thawing processes (Oleson et al., 2013), a revised numerical solution of the Richards equation to update the hydrology scheme (Zeng & Decker, 2009), an advanced representation of the thermal and hydraulic properties of soil organic matter to reduce the simulated warm bias (Nicolsky et al., 2007), the deepening (15 layers, ~50 m) of the soil column to represent the thermal inertia from the cold deep permafrost (Alexeev et al., 2007), and an update of the cold region hydrological processes for moderating the simulated dry surface organic soil (Swenson et al., 2012). The soil freezing begins as the soil temperature < 0 °C and soil liquid water > the maximum unfrozen water content, while the soil thawing begins as the soil temperature > 0 °C and the soil ice content > 0. A freezing-point depression equation was employed to compute the maximum soil unfrozen water content to permit the coexistence of liquid water and ice over a certain range of soil temperature < 0 °C (Niu & Yang, 2006). These improvements have been demonstrated to be much conducive to the model's simulation of frozen ground conditions (Koven et al., 2013; Lawrence et al., 2012). The model has been widely employed to study soil water and heat processes and permafrost dynamics (Gao et al., 2016; Guo & Wang, 2013; Lawrence et al., 2012; Luo et al., 2017; Wang et al., 2016).

2.3. Experimental Design

Four simulation experiments were carried out using CLM4.5, each driven by one of the forcing data sets: CFSR, ERA-I, MERRA, and CRUNCEP. The atmospheric inputs required by CLM4.5 include the air temperature, precipitation, air pressure, wind speed, specific humidity, and downward shortwave radiation. The default surface and soil texture data sets in CLM4.5 were used in this study. The four simulations were carried out on a global scale at a spatial resolution of 0.5° × 0.5°, with a simulation period from 1979 to 2009. The daily step was set as the temporal resolution of the model output.

For model initialization, the model was cyclically spun up for 100 years with the CRUNCEP forcing data set in 1979. Using the final model state as the initial conditions, the model was then cyclically run for 30, 30, 40, and 0 years with the CFSR, ERA-I, MERRA, and CRUNCEP forcing data sets in 1979, respectively. The interannual variations in the ground temperature were smaller than 0.002 °C at the end of all these initialization runs, indicating the model arriving at the stabilization state. The final state of each initialization run was saved and taken as the new initial conditions for performing the corresponding transient simulation from 1979 to 2009.

2.4. Methods

Similar to the works of Guo and Wang (2014) and Wang et al. (2015), three variables (freeze start date, freeze end date, and freeze duration) were used to express the changes in the soil freeze/thaw cycle. The near-surface freeze start (end) date was identified as the date (Julian date) when the daily ground temperature transited from above (below) 0 °C to below (above) 0 °C. To avoid the impact of the random changes in the ground temperature on the identification of the freeze start and end dates, it was assumed that if three consecutive days met the criteria that the ground temperature was below (above) 0 °C, the first day of these three consecutive days was identified as the freeze start (end) date (Guo et al., 2011b; Guo & Wang, 2014). The freeze duration was calculated as days between freeze start date and freeze end date within a calendar year.

The Nash-Sutcliffe efficiency (NSE) (Nash & Sutcliffe, 1970), temporal correlation coefficient, and linear trend were used to quantitatively assess the level of agreement between the simulations and observations. The NSE is calculated as
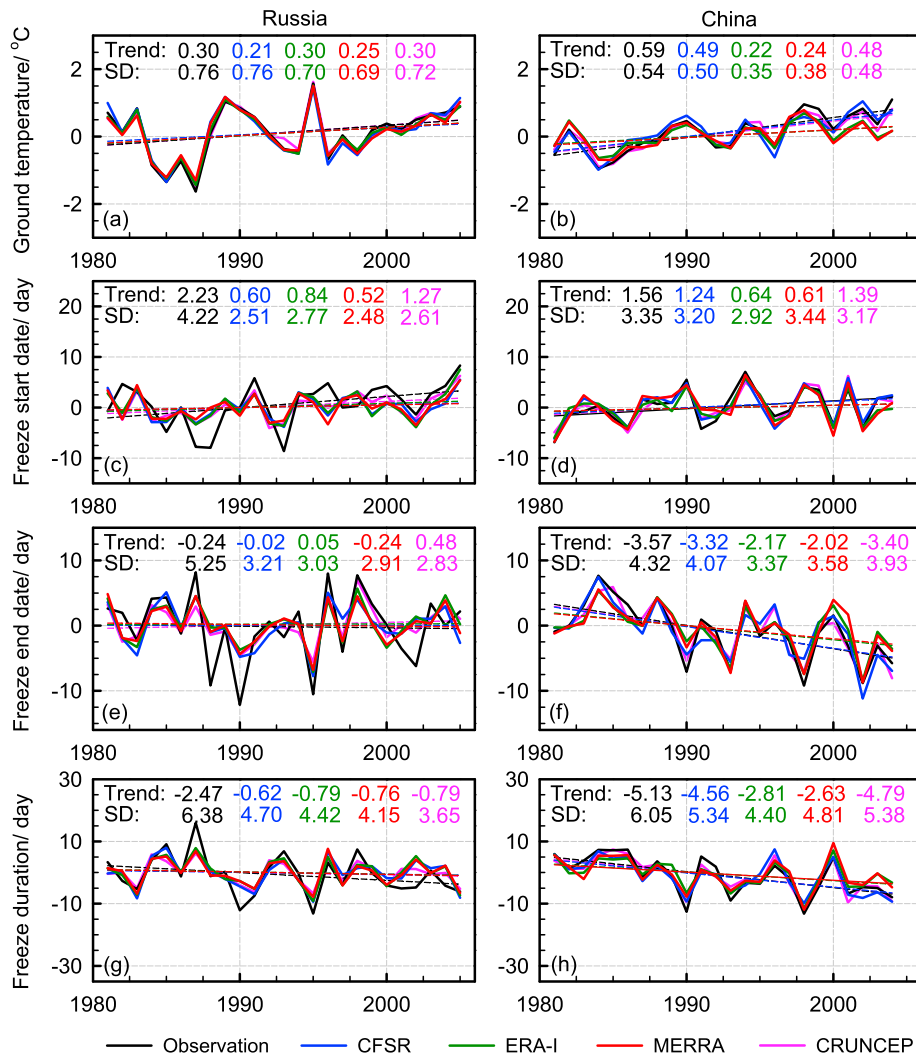
Figure 2. Comparison of the simulated changes (1981–2005) in (a and b) ground temperature, (c and d) freeze start date, (e and f) freeze end date, and (g and h) freeze duration of the CFSR, ERA-I, MERRA, and CRUNCEP data sets with the observational results in Russia (a, c, e, and g) and in China (b, d, f, and h), relative to the 1981–2000 data. The dashed lines represent regression lines of the corresponding time series. The linear trends (trend) and standard deviation (SD) in the simulated and observed results are given at the top of each panel.

$$\text{NSE} = 1 \frac{\sum_{t=1}^{T}(Q_{\text{obs}} - Q_{\text{sim}})^2}{\sum_{t=1}^{T}(Q_{\text{obs}} - Q_{\text{obs}})^2}$$

where Q_{obs} denotes observations, Q_{sim} denotes simulations, and T denotes the total number of samples.

The NSE expresses how closely the plot of the simulated and observed values fits the 1:1 line, which is sensitive to the outliers. The NSE has a range of $-\infty$ to 1; the simulated values are more accurate when the NSE statistic is closer to 1. In addition to the NSE, the temporal correlation coefficient is also used to separately assess the similarities of temporal variations in the simulated and observed results. The linear trend is taken as the slope of the linear fit that is calculated based on the least squares regression (Guo & Wang, 2012; Guo et al., 2018; Zhou et al., 2016; Qin et al., 2009), and its statistical significance is assessed using the Student's t test.

3. Results

3.1. Validation of the Models

The simulated variations in the ground temperature from the four simulations fit closely to the respective observations (Figures 2a and 2b). Across the four simulations and two countries, the NSEs are between

Table 2
Statistics of the Similarities Between the Simulated and Observed Changes in the Ground Temperature and Near-Surface Soil Freeze/Thaw Cycle[a]

Index	Change in ground temperature (°C) (1979–2009) CFSR, ERA-I, MERRA, CRUNCEP	Change in near-surface soil freeze/thaw cycle (m) (1979–2009)		
		Freeze start date CFSR, ERA-I, MERRA, CRUNCEP	Freeze end date CFSR, ERA-I, MERRA, CRUNCEP	Freeze duration CFSR, ERA-I, MERRA, CRUNCEP
Correlation coefficient (Russia)	0.98, 0.99, 0.98, 0.99	0.57, 0.64, 0.47, 0.66	0.72, 0.71, 0.76, 0.81	0.79, 0.78, 0.77, 0.82
Nash-Sutcliffe efficiency (Russia)	0.96, 0.98, 0.96, 0.98	0.31, 0.40, 0.19, 0.43	0.51, 0.49, 0.53, 0.58	0.61, 0.58, 0.56, 0.60
Correlation coefficient (China)	0.93, 0.88, 0.85, 0.97	0.93, 0.92, 0.87, 0.92	0.90, 0.92, 0.92, 0.95	0.91, 0.91, 0.90, 0.94
Nash-Sutcliffe efficiency (China)	0.87, 0.69, 0.67, 0.94	0.87, 0.85, 0.74, 0.84	0.82, 0.83, 0.82, 0.89	0.83, 0.79, 0.79, 0.88

Note. The four simulations are based on the CFSR, ERA-I, MERRA, and CRUNCEP data sets.
[a]All correlation coefficients with the statistically significance of 95%.

0.67 and 0.98, and temporal correlation coefficients are between 0.85 and 0.99 (Table 2). Part of the four simulations also replicate the observed trend in the ground temperature. The ERA-I- and CRUNCEP-based simulations produce the same trend of 0.30 °C decade^{-1}, which is equal to that of the observations in Russia. The CFSR- and CRUNCEP-based simulations also produce trends of 0.49 and 0.48 °C decade^{-1}, which are close to, but slightly lower than, the observational ground temperature trend (0.59 °C decade^{-1}) in China. The differences in the performances of the four simulations are related to different atmospheric forcing data sets used to drive the model.
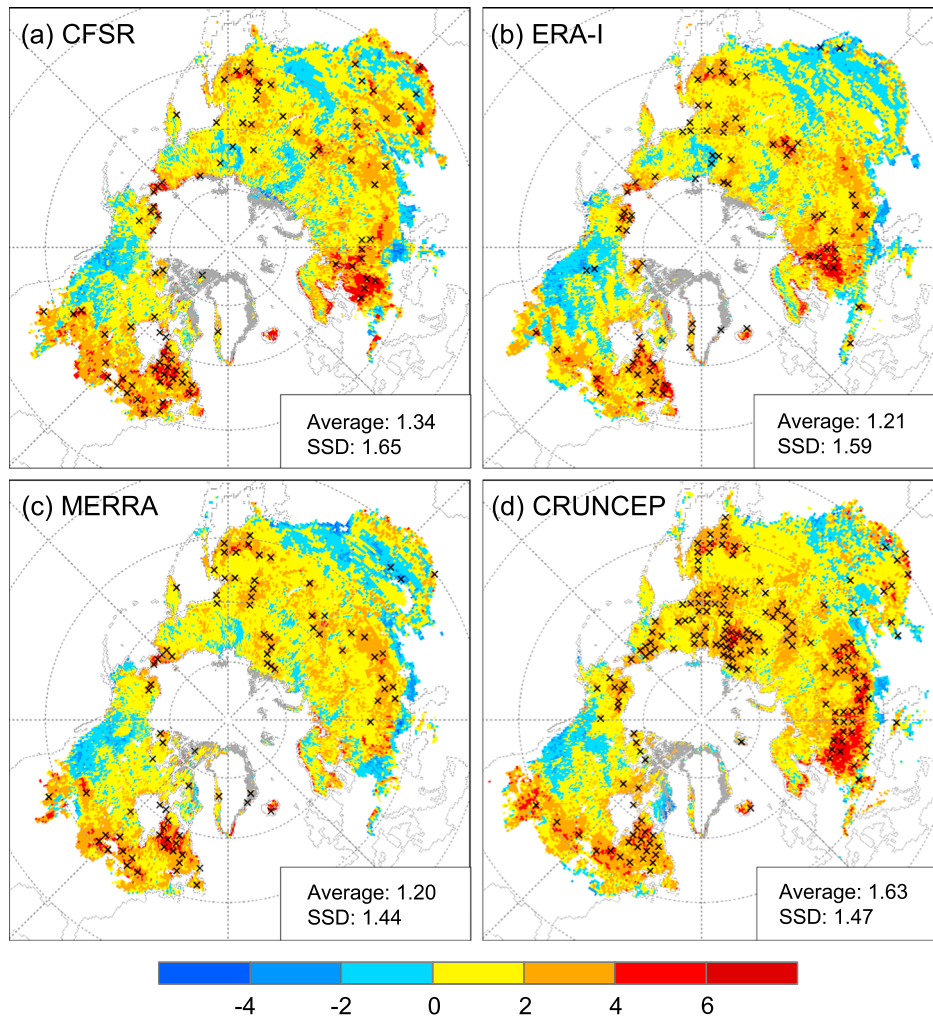
The simulated variations in the near-surface soil freeze start date, freeze end date, and freeze duration from the four simulations also agree well with the respective observational variations, but the performances are weaker than those of the simulated ground temperature (Figures 2a–2h). For the freeze start date, across the four simulations and two countries, the NSEs are between 0.19 and 0.87, and the temporal correlation coefficients are between 0.47 and 0.93 (Table 2). The CRUNCEP-based simulation produces trends of 1.27 (Russia) and 1.39 days decade^{-1} (China), which are comparable with the observed trends of 2.23 (Russia) and 1.56 days decade^{-1} (China). For the freeze end date, the NSEs are between 0.49 and 0.89, and the temporal correlation coefficients are between 0.71 and 0.95 across the four simulations and two countries (Table 2). The MERRA-based simulation produces the equivalent trend (−0.24 day decade^{-1}) to the observed trend in Russia, and the CRUNCEP-based simulation produces a close to but slightly larger trend (−3.40 days decade^{-1}) than that (−3.57 days decade^{-1}) in the observational data from China. The NSE and temporal correlation coefficient regarding the freeze duration range from 0.56 to 0.88 and from 0.77 to 0.94, respectively, across the four simulations and two countries (Table 2). The CRUNCEP-based simulation produces close to but larger trends in the freeze duration than those of the observations in both countries.

Notably, the performances of four simulations are close to each other. Overall, the CRUNCEP-based simulation's performance is relatively superior to the other three simulations in terms of correlation coefficient and NSE between simulated and observed results shown in Table 2. This means that the CRUNCEP forcing data sets can be preferentially selected as the basic atmospheric forcing data set for future application, that is, prediction.

It is noted that the simulation performance of the model for predicting the variations in the freeze/thaw cycle is more accurate in China than in Russia, according to our validation (Table 2). The reason might be related to the uncertainties in snow simulation, which is discussed in the section 4. More snow may bring larger simulation biases in Russia relative to China. It should be mentioned that our validation only focuses on the regions in Eurasia, not including North American due to the unavailability of observations there. Thus, there is no direct evidence assessing the accuracy of the simulated results in North American. Because the same model and atmospheric forcing data sets are used in these two regions, the validation in Eurasia could give an indication to the accuracy of simulated results in North American. This indication may be limited because the same model or atmospheric forcing data set may have different performances in different regions.

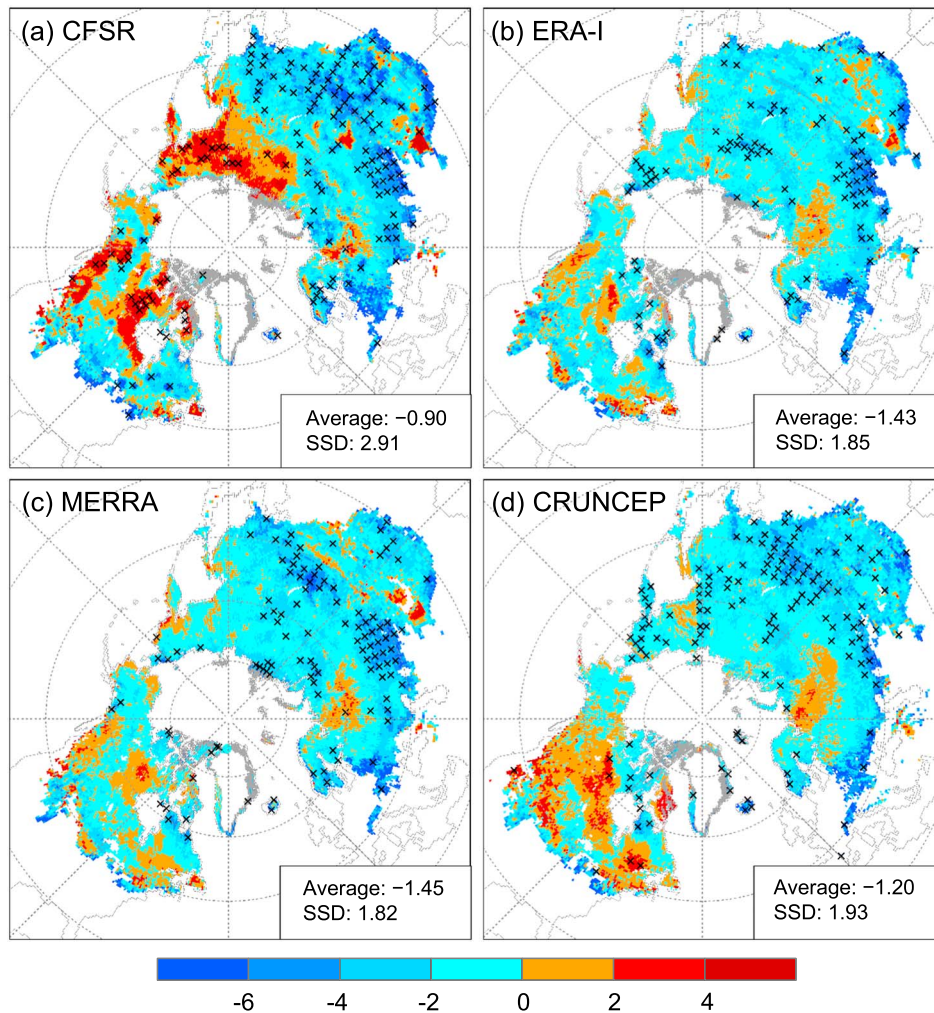### 3.2. Changes in the Near-Surface Soil Freeze/Thaw Cycle

The four simulations produce similar spatial patterns of the trends in the simulated near-surface soil freeze start date, with an exception that CRUNCEP-based simulation shows larger trends in the eastern part of Siberia, Russia (Figures 3a–3d). The similarities are not surprised because the validated performances are

Figure 3. Spatial distribution of the trend (day decade^{-1}) in the simulated near-surface soil freeze start date from the simulations based on the (a) CFSR, (b) ERA-I, (c) MERRA, and (d) CRUNCEP data sets from 1979 to 2009. The gray grids represent the places where the near-surface soil never thaws over the course of at least 1 year between 1979 and 2009. These gray grids are not considered when the area-averaged values are calculated. Areas with significance level exceeding 95% are denoted with "plus" sign. The area-averaged (average) trends and spatial standard deviation (SSD) of the trends are given in the bottom right corner of panels (a), (b), (c), and (d).

close to each other for the four simulations (Table 2). The majority of the regions show delaying (positive) trends in the freeze start date, except for some regions, such as the western Canada and the Tibetan Plateau and its adjacent areas, where advancing (negative) trends are present. Among the four simulations, the CRUNCEP-based simulation has the greatest area-averaged trend of 1.63 (spatial standard deviation [SSD]: 1.47) days decade^{-1}, followed by CFSR-based simulation (1.34 [SSD: 1.65] days decade^{-1}), ERA-I-based simulation (1.21 [SSD: 1.59] days decade^{-1}), and MERRA-based simulation (1.20 [SSD: 1.44] days decade^{-1}).

For the near-surface soil freeze end date, the four simulations consistently show that majority of the regions have advancing trends; however, delaying trends are present in some regions, such as western and central Canada, the Labrador Plateau in Canada, and the East European Plain (Figures 4a–4d). Different from the other three simulations, the CFSR-based simulation also shows additional regions with distinctly delaying trends in the eastern part of Siberia, Russia (Figure 4a). The simulated freeze end date mostly occurs in May and June in the eastern part of Siberia, Russia (not shown). The CFSR air temperature shows cooling or weak warming from 1979 to 2009 in the eastern part of Siberia, Russia, whereas the ERA-I, MERRA, and CRUNCEP air temperatures show significant warming in those locations (not shown). Thus, different changes in air temperature are responsible for the inconsistent freeze end date trends in the eastern part of Siberia, Russia, among the four simulations. The four simulations have area-averaged trends of −0.90 (SSD: 2.91) (CFSR), −1.43 (SSD: 1.85) (ERA-I), −1.45 (SSD: 1.82) (MERRA), and −1.20 (SSD: 1.93)
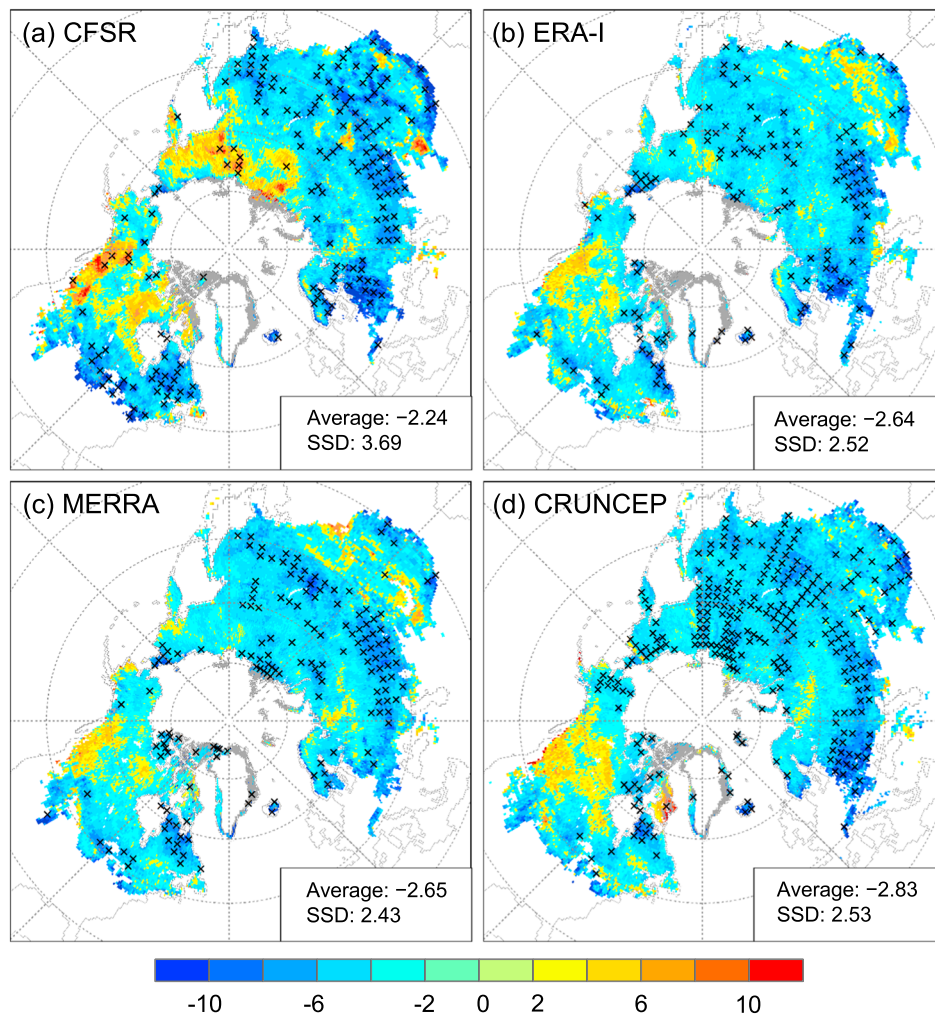
Figure 4. Similar to Figure 3 but for the near-surface soil freeze end date.

(CRUNCEP) days decade^{-1}. The small area-averaged advancing trend of CFSR-based simulation results from the evident delaying trends in the eastern part of Siberia, Russia, and the western and central Canada.

The spatial patterns of the near-surface soil freeze duration are largely similar to those of the freeze end date (Figure 5). The majority of the regions show a shortening freeze duration, leaving some regions such as western and central Canada and the East European Plain with extending duration trends. In addition, only CFSR-based simulation shows apparent extending duration trends in the eastern part of Siberia, Russia among the four simulations. These similarities indicate that the changes in the freeze duration are mostly related to the changes in the freeze end date relative to the freeze start date.

The area-averaged trends of the near-surface soil freeze duration are −2.24 (SSD: 3.69), −2.64 (SSD: 2.52), −2.65 (SSD: 2.43), and −2.83 (SSD: 2.53) days decade^{-1} for the CFSR-, ERA-I-, MERRA-, and CRUNCEP-based simulations, respectively (Figure 5). For the ERA-I- and MERRA-based simulations, the area-averaged earlier trends in the freeze end date are greater than the later trends in the freeze start date (Figures 3 and 4), which indicates that the freeze end date contributes the more to the area-averaged shortening of the freeze duration. In contrast, for the CFSR- and CRUNCEP-based simulations, the greater delay in the freeze end date in western and central Canada and the eastern part of Siberia, Russia, causes the area-averaged advance in the freeze end date to be less influential on the area-averaged shortening freeze duration than the delay in the freeze start date.

The four simulations show very similar interannual variations in all the three variables with respect to the soil freeze/thaw cycle during the period 1979–2009 (Figure 6). For the period from 1979 to 2009, the freeze start

Figure 5. Similar to Figure 3 but for the near-surface soil freeze duration.

date delayed by a range of 3.72–5.05 days, with one standard deviation of 0.54 days across the four simulations (Table 3). In contrast, the freeze end date advanced by a range of 2.79–4.50 days, with one standard deviation of 0.69 days across the four simulations. The delay in the freeze start date combined with the advance in the freeze end date results in a shortening of the freeze duration by a range of 6.94–8.77 days, with one standard deviation of 0.67 days across the four simulations.

3.3. Relation of the Change in the Freeze Duration With Latitude and Air Temperature

Of the four simulations, the simulations based on CFSR, MERRA, and CRUNCEP show that the shortening trend in the freeze duration generally weakens with increasing latitude, from 27.75°N to 75.25°N, whereas the ERA-I-based simulation shows a slight strengthening in the shortening trend of the freeze duration (Figure 7). Specifically, the four simulations show that the shortening trend in the freeze duration first consistently weakens with increasing latitude, from 27.75°N to about 36.75°N, and then strengthens with increasing latitude, from about 36.75°N to 47.25°N. With latitude increasing from about 47.25°N to 67.75°N, the shortening trend steadily weakens and then strengthens with a further increase in latitude, until the 75.25°N; however, the CFSR-based simulation shows a weakening shortening trend and changes to an extending trend with increasing latitude, from about 67.75°N to 75.25°N. This exception is mainly caused by the CFSR-based simulation producing the extending trends in the eastern part of Siberia, Russia (Figure 5a).

The relationship between freeze duration and seasonal air temperature changes is quantitatively analyzed in terms of CRUNCEP-based simulation (Figure 8). The freeze duration shows a significantly negative correlation
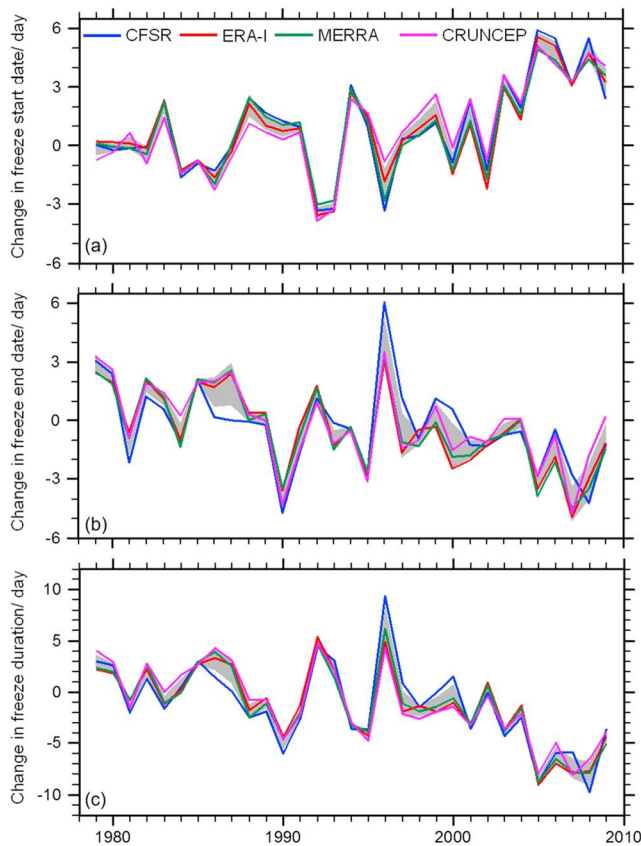
Figure 6. The temporal changes in the area-averaged freeze start date (a), freeze end date (b), and freeze duration (c) from the simulations based on the CFSR, ERA-I, MERRA, and CRUNCEP data sets from 1979 to 2009, relative to the 1981–2000 data. The shaded areas in the three panels represent one standard deviation across the results of the simulations based on the four atmospheric forcing data sets.

with air temperature change in almost all study areas in spring and autumn. For comparison, this correlation is distinctly weak and insignificant in summer and winter. This is consistent with our general knowledge that the freeze start and end dates are mostly related to air temperatures in autumn and spring. Differently, in the northern Canada, the freeze duration is significantly correlated with air temperature in summer. This is because freeze end date in the northern Canada occurs in summer rather than in spring (not shown). It should be noted that the correlations between the freeze duration and air temperature are more significant in spring than in autumn. This indicates that the spring change in the air temperature is more responsible for the shortening of the freeze duration than that in autumn.

4. Discussions

Numerical model was used to simulate the past long-term changes in the near-surface soil freeze/thaw cycle, with a possible application for predicting future changes. The land surface model of CLM4.5 was employed in this study. The multiple reanalysis-based forcing data sets were used for evaluating the uncertainties in the simulated results from different forcing data sets. In situ observations from 112 weather stations in Russia and 187 weather stations in China were used to validate the simulated results at higher and lower latitudes, respectively. The results show that the simulated changes in the ground temperature, the freeze start and end dates, and the freeze duration agree closely with the observations. This indicates that the numerical simulation is well suited for estimates of the long-term changes in the near-surface soil freeze/thaw cycle.

The simulated results are comparable with those from satellite monitoring and measurements. The previous results using a satellite remote sensing method show an earlier spring thawing at a rate of -1.50 days decade^{-1} and a decreasing annual freeze duration at a rate of -1.90 days decade^{-1} in the Northern Hemisphere from 1979 to 2008 (Kim et al., 2012), and a mean advance of -1.2 days decade^{-1} in the spring first leaf date in the Northern Hemisphere from 1955 to 2002 (Schwartz et al., 2006). As a comparison, our simulated freeze end date advances by -1.25 ± 0.22 days decade^{-1} and freeze duration shortens at -2.59 ± 0.22 days decade^{-1} from 1979 to 2009. Previous observation-based studies also showed a similar advance (-1.46 days decade^{-1}) in the spring thawing and delay (1.20 days decade^{-1}) in the autumn freezing date in the land area of the Northern Hemisphere from 1960 to 2009 (Burrows et al., 2011), and decrease (-2.50 ± 0.04 days decade^{-1}) in the near-surface freeze duration in China from 1956 to 2006 (Wang et al., 2015).

In addition to the different atmospheric forcing data sets, snow simulations may be another source of uncertainty in the simulated results. The seasonal snow cover has significant influence on the ground thermal regime (Zhang, 2005). Although the snow model in CLM4.5 has had many modifications (Lawrence et al.,

Table 3
Present-Day Climatology, Trend, and Change for the Ground Temperature, Freeze Start Date, Freeze End Date, and Freeze Duration[a]

| Variable	Present day (1981–2000)	Trend in 1979–2009 (per decade)	Change in 1979–2009
Ground temperature (°C)	-4.56 ± 0.51	0.42 ± 0.002	1.31 ± 0.007
Freeze start date (day)	285.98 ± 0.41	1.35 ± 0.17	4.17 ± 0.54
Freeze end date (day)	124.46 ± 2.17	-1.25 ± 0.22	-3.86 ± 0.69
Freeze duration (day)	203.48 ± 2.24	-2.59 ± 0.22	-8.03 ± 0.67

[a]The range of uncertainty is one standard deviation across the results of the simulations based on the four atmospheric forcing data sets.
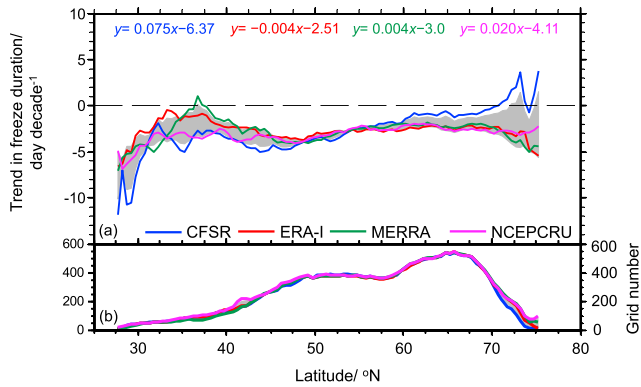
Figure 7. (a) Change of the latitudinal mean trend in the freeze duration from 1979 to 2009 with increasing latitudes and (b) the number of simulation grids for the latitudinal mean in each latitude bin. The shaded areas represent one standard deviation across the results of the simulations based on four atmospheric forcing data sets.

2011), deficiencies of snow process parameterization still exist in the model. For example, when the total precipitation is inputted, the model separates snowfall and rainfall according to an empirical formulation based on the air temperature, which may introduce some biases in the simulation of the snow cover. When the observed snow depth and satellite snow cover were used to evaluate the simulation results from CLM4.0, it was found that the snow depth was underestimated and early snowmelt was predicted (Toure et al., 2016). Wang et al. (2016) also found that the CLM4.5-simulated snow water equivalent peaked much earlier than observed in eastern Siberia and the western United States. The biases in the simulated timing of snow melting may affect model estimates of the near-surface soil freeze end date and contribute to uncertainties in the results.

This study shows that the shortening of the soil freeze duration statistically significantly correlates with air temperature in spring and autumn. Smith et al. (2004) also found that the thaw (freeze) timing was negatively (positively) correlated with spring (autumn) air
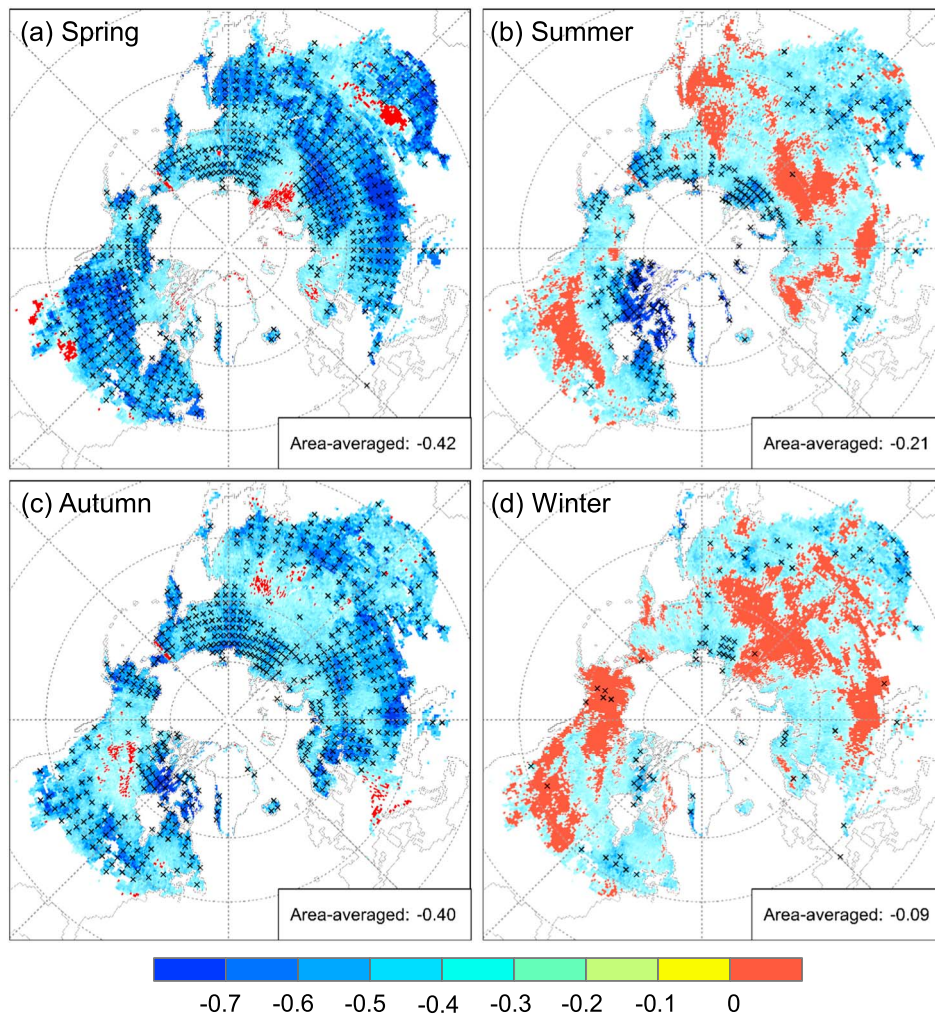
Figure 8. Spatial distribution of the temporal correlation coefficients between the near-surface soil freeze duration and the surface air temperature from the simulation based on the CRUNCEP data set in (a) spring, (b) summer, (c) autumn, and (d) winter from 1979 to 2009. Areas with significance level exceeding 95% are denoted with "plus" sign. The area-averaged values are given in the bottom right corner of panels (a), (b), (c), and (d).

temperature in the high northern latitude land areas. This study further shows that the spring air temperature is the dominant factor influencing the freeze duration in terms of CRUNCEP-based simulation, relative to the autumn air temperature. In addition, it is indicated that substantial heat islands, which are a result of urbanization, contribute to the change in the near-surface soil freeze (Wang et al., 2015). Besides, it is found that both the winter North Atlantic Oscillation and the February Arctic Oscillation correspond to the near-surface soil freeze duration due to their effect on the surface air temperature (Wang et al., 2015). More factors associated with changes in the near-surface soil freeze/thaw cycle require further research in the future.

5. Conclusions

The changes in the near-surface soil freeze/thaw cycle from 1979 to 2009 were simulated using CLM4.5, driven by four reanalysis-based atmospheric forcing data sets. The simulated long-term temporal changes in the near-surface soil temperature, freeze start date, freeze end date, and freeze duration are validated to be in close agreement with the observational data; the temporal correlation coefficients are between 0.47 and 0.99, and the NSEs are between 0.19 and 0.98. The linear trends in these four freeze/thaw cycle variables can also be captured by parts of the four simulations. It is found that the simulated results are more reasonable in China, at lower latitudes, than those in Russia, at higher latitudes. Overall, among the four simulations, the CRUNCEP-based simulation produces the results that are the most similar to the observational data. We therefore suggest that the CRUNCEP data set can be preferentially considered as the basic atmospheric forcing data set for future prediction.

The simulated freeze start date was averagely delayed by 4.17 days over the four simulations, whereas the freeze end date was averagely advanced by 3.86 days. The delay in the freeze start date, which was combined with the advance in the freeze end date, resulted in an average shortening of the freeze duration of 8.03 days from 1979 to 2009. The different atmospheric forcing data sets result in uncertainties (one standard deviation) of 0.54, 0.69, and 0.67 days in the changes in freeze start date, freeze end date, and freeze duration, respectively.

These results give an insight into how well numerical model is used to estimate the long-term changes of the near-surface soil freeze/thaw cycle, which are considered to be useful for prediction of future freeze/thaw dynamics. The simulated changes in the timing and duration of the soil freeze are comparable to those from both the in situ observations and satellite remote sensing monitoring. Atmospheric forcing data sets and snow simulations contribute to the uncertainties in the simulated results. Historically, research on long-term changes in the soil freeze/thaw cycle has moved from direct measurements at the local scale in some countries (Anandhi et al., 2013; Henry, 2008; Menzel et al., 2003; Wang et al., 2015), to monitoring with satellite remote sensing on the regional and global scales (Kim et al., 2012; McDonald et al., 2004; Smith et al., 2004; Zhang et al., 2003). The present study performed a numerical simulation of the change in the timing and duration of the annual soil freeze in the Northern Hemisphere from 1979 to 2009. Continued work is planned that will predict the future near-surface soil free/thaw cycle dynamics using the CLM driven by climatology from reanalysis-based climatology combined with anomalies from the climate models of the fifth phase of the Coupled Model Intercomparison Project.

References

Alexeev, V. A., Nicolsky, D. J., Romanovsky, V. E., & Lawrence, D. M. (2007). An evaluation of deep soil configurations in the CLM3 for improved representation of permafrost. *Geophysical Research Letters*, *34*, L09502. https://doi.org/10.1029/2007GL029536

Anandhi, A., Perumal, S., Gowda, P., Knapp, M., Hutchinson, S., Harrington, J. Jr., et al. (2013). Long-term spatial and temporal trends in frost indices in Kansas, USA. *Climatic Change*, *120*, 169–181.

Burrows, M. T., Schoeman, D. S., Buckley, L. B., Moore, P., Poloczanska, E. S., Brander, K. M., et al. (2011). The pace of shifting climate in marine and terrestrial ecosystems. *Science*, *334*(6056), 652–655. https://doi.org/10.1126/science.1210288

Chen, B., Luo, S., Lü, S., Zhang, Y., & Ma, D. (2014). Effects of the soil freeze-thaw process on the regional climate of the Qinghai-Tibet Plateau. *Climate Research*, *59*, 243–257.

Chen, L., Ma, Z., Zhao, T., Li, Z., & Li, Y. (2017). Simulation of the regional climatic effect of irrigation over the Yellow River Basin. *Atmospheric and Oceanic Science Letters*, *10*(4), 291–297.

Cheng, G., & Wu, T. (2007). Responses of permafrost to climate change and their environmental significance, Qinghai–Tibet Plateau. *Journal of Geophysical Research*, *112*, F02S03. https://doi.org/10.1029/2006JF000631

Dee, D., et al. (2011). The ERA-Interim reanalysis: Configuration and performance of the data assimilation system. *Quarterly Journal of the Royal Meteorological Society*, *137*(656), 553–597. https://doi.org/10.1002/qj.828

Fan, K., Xie, Z., & Xu, Z. (2016). Two different periods of high dust weather frequency in northern China. *Atmospheric and Oceanic Science Letters*, *9*(4), 263–269. https://doi.org/10.1080/16742834.2016.1176300

Flanner, M. G., Zender, C. S., Randerson, J. T., & Rasch, P. J. (2007). Present-day climate forcing and response from black carbon in snow. *Journal of Geophysical Research*, *112*, D11202. https://doi.org/10.1029/2006JD008003

Gao, Y. (2017). Shift of the principal mode of Pan-Asian monsoon summer precipitation in terms of spatial pattern. *Atmospheric and Oceanic Science Letters*, *10*, 221–227.

Gao, X., Shi, Y., & Giorgi, F. (2016). Comparison of convective parameterizations in RegCM4 experiments over China with CLM as the land surface model. *Atmospheric and Oceanic Science Letters*, *9*(4), 246–254.

Guo, D. L., & Wang, H. J. (2012). The significant climate warming in the northern Tibetan Plateau and its possible causes. *International Journal of Climatology*, *32*(12), 1775–1781. https://doi.org/10.1002/joc.2388

Guo, D. L., & Wang, H. J. (2013). Simulation of permafrost and seasonally frozen ground conditions on the Tibetan Plateau, 1981–2010. *Journal of Geophysical Research: Atmospheres*, *118*, 5216–5230. https://doi.org/10.1002/jgrd.50457

Guo, D. L., & Wang, H. J. (2014). Simulated change in the near-surface soil freeze/thaw cycle on the Tibetan Plateau from 1981 to 2010. *Chinese Science Bulletin*, *59*(20), 2439–2448. https://doi.org/10.1007/s11434-014-0347-x

Guo, D. L., & Wang, H. J. (2017). Simulated historical (1901–2010) changes in the permafrost extent and active layer thickness in the Northern Hemisphere. *Journal of Geophysical Research: Atmospheres*, *122*, 12,285–12,295. https://doi.org/10.1002/2017JD027691

Guo, D. L., Wang, H. J., & Wang, A. H. (2017). Sensitivity of historical simulation of the permafrost to different atmospheric forcing datasets from 1979 to 2009. *Journal of Geophysical Research: Atmospheres*, *122*, 12,269–12,284. https://doi.org/10.1002/2017JD027477

Guo, D. L., Yang, M. X., & Wang, H. J. (2011a). Sensible and latent heat flux response to diurnal variation in soil surface temperature and moisture under different freeze/thaw soil conditions in the seasonal frozen soil region of the central Tibetan Plateau. *Environment and Earth Science*, *63*(1), 97–107. https://doi.org/10.1007/s12665-010-0672-6

Guo, D. L., Yang, M. X., & Wang, H. J. (2011b). Characteristics of land surface heat and water exchange under different soil freeze/thaw conditions over the central Tibetan Plateau. *Hydrological Processes*, *25*(16), 2531–2541. https://doi.org/10.1002/hyp.8025

Guo, D. L., Li, D., & Hua, W. (2018). Quantifying air temperature evolution in the permafrost region from 1901 to 2014. *International Journal of Climatology*, *38*(1), 66–76. https://doi.org/10.1002/joc.5161

Henry, H. A. L. (2008). Climate change and soil freezing dynamics: Historical trends and projected changes. *Climatic Change*, *87*(3-4), 421–434. https://doi.org/10.1007/s10584-007-9322-8

Kalnay, E., Kanamitsu, M., Kistler, R., Collins, W., Deaven, D., Gandin, L., et al. (1996). The NCEP/NCAR 40-Year Reanalysis Project. *Bulletin of the American Meteorological Society*, *77*(3), 437–471. https://doi.org/10.1175/1520-0477(1996)077%3C0437:TNYRP%3E2.0.CO;2

Kim, Y., Kimball, J. S., McDonald, K. C., & Glassy, J. (2011). Developing a global data record of daily landscape freeze/thaw status using satellite passive microwave remote sensing. *IEEE Transactions on Geoscience and Remote Sensing*, *49*, 949–960.

Kim, Y., Kimball, J. S., Zhang, K., & McDonald, K. C. (2012). Satellite detection of increasing Northern Hemisphere non-frozen seasons from 1979 to 2008: Implications for regional vegetation growth. *Remote Sensing of Environment*, *121*, 472–487. https://doi.org/10.1016/j.rse.2012.02.014

Kimball, J. S., McDonald, K. C., Running, S. W., & Frolking, S. E. (2004). Satellite radar remote sensing of seasonal growing seasons for boreal and subalpine evergreen forests. *Remote Sensing of Environment*, *90*(2), 243–258. https://doi.org/10.1016/j.rse.2004.01.002

Kimball, J. S., McDonald, K. C., & Zhao, M. (2006). Spring thaw and its effect on terrestrial vegetation productivity in the western Arctic observed from satellite microwave and optical remote sensing. *Earth Interactions*, *10*(21), 1–22. https://doi.org/10.1175/EI187.1

Koven, C. D., Riley, W. J., & Stern, A. (2013). Analysis of permafrost thermal dynamics and response to climate change in the CMIP5 Earth system models. *Journal of Climate*, *26*(6), 1877–1900. https://doi.org/10.1175/JCLI-D-12-00228.1

Kurganova, I., Teepe, R., & Loftfield, N. (2007). Influence of freeze–thaw events on carbon dioxide emission from soils at different moisture and land use. *Carbon Balance and Management*, *2*(1), 2. https://doi.org/10.1186/1750-0680-2-2

Lawrence, P. J., & Chase, T. N. (2007). Representing a MODIS consistent land surface in the Community Land Model (CLM 3.0). *Journal of Geophysical Research*, *112*, G01023. https://doi.org/10.1029/2006JG000168

Lawrence, P. J., & Chase, T. N. (2010). Investigating the climate impacts of global land cover change in the community climate system model. *International Journal of Climate*, *30*, 2066–2087.

Lawrence, D. M., Oleson, K. W., Flanner, M. G., Thornton, P. E., Swenson, S. C., Lawrence, P. J., et al. (2011). Parameterization improvements and functional and structural advances in version 4 of the Community Land Model. *Journal of Advances in Modeling Earth Systems*, *3*(3) M03001. https://doi.org/10.1029/2011MS000045

Lawrence, D. M., Slater, A. G., & Swenson, S. C. (2012). Simulation of present-day and future permafrost and seasonally frozen ground conditions in CCSM4. *Journal of Climate*, *25*(7), 2207–2225. https://doi.org/10.1175/JCLI-D-11-00334.1

Li, Q., & Chen, H. S. (2013). Variation of seasonal frozen soil in East China and their association with monsoon activity under the background of global warming. *Climatic Change Research Letters*, *02*(02), 47–53. https://doi.org/10.12677/CCRL.2013.22008

Li, X., Jin, R., Pan, X., Zhang, T., & Guo, J. (2012). Changes in the near-surface soil freeze–thaw cycle on the Qinghai-Tibetan Plateau. *International Journal of Applied Earth Observation and Geoinformation*, *17*, 33–42. https://doi.org/10.1016/j.jag.2011.12.002

Luo, S., Fang, X., Lyu, S., Zhang, Y., & Chen, B. (2017). Improving CLM4. 5 simulations of land-atmosphere exchanges during freeze-thaw processes on the Tibetan Plateau. *Journal of Meteorology Research*, *31*(5), 916–930. https://doi.org/10.1007/s13351-017-6063-0

Mao, J., Shi, X., Thornton, P. E., Hoffman, F. M., Zhu, Z., & Myneni, R. B. (2013). Global latitudinal-asymmetric vegetation growth trends and their driving mechanisms: 1982–2009. *Remote Sensing*, *5*(12), 1484–1497. https://doi.org/10.3390/rs5031484

McDonald, K. C., Kimball, J. S., Njoku, E., Zimmermann, R., & Zhao, M. (2004). Variability in springtime thaw in the terrestrial high latitudes: Monitoring a major control on the biospheric assimilation of atmospheric CO2 with spaceborne microwave remote sensing. *Earth Interactions*, *8*(20), 1–23. https://doi.org/10.1175/1087-3562(2004)8%3C1:VISTIT%3E2.0.CO;2

Menzel, A., Jakobi, G., Ahas, R., Scheifinger, H., & Estrella, N. (2003). Variations of the climatological growing season (1951–2000) in Germany compared with other countries. *International Journal of Climatology*, *23*(7), 793–812. https://doi.org/10.1002/joc.915

Mitchell, T. D., & Jones, P. D. (2005). An improved method of constructing a database of monthly climate observations and associated high-resolution grids. *International Journal of Climatology*, *25*(6), 693–712. https://doi.org/10.1002/joc.1181

Nash, J. E., & Sutcliffe, J. V. (1970). River flow forecasting through conceptual models. Part I: A discussion of principles. *Journal of Hydrology*, *10*(3), 282–290. https://doi.org/10.1016/0022-1694(70)90255-6

Nicolsky, D. J., Romanovsky, V. E., Alexeev, V. A., & Lawrence, D. M. (2007). Improved modeling of permafrost dynamics in a GCM land-surface scheme. *Geophysical Research Letters*, *34*, L08501. https://doi.org/10.1029/2007GL029525

Niu, G. Y., & Yang, Z. L. (2006). Effects of frozen soil on snowmelt runoff and soil water storage at a continental scale. *Journal of Hydrometeorology*, *7*(5), 937–952. https://doi.org/10.1175/JHM538.1

Oleson, K. W., Bonan, G. B., Feddema, J., Vertenstein, M., & Grimmond, C. S. B. (2008). An urban parameterization for a global climate model. Part I: Formulation and evaluation for two cities. *Journal of Applied Meteorology and Climatology*, *47*(4), 1038–1060. https://doi.org/10.1175/2007JAMC1597.1

Oleson, K., Lawrence, D. M., Bonan, G. B., Drewniak, B., Huang, M., Koven, C. D., et al. (2013). *Technical description of version 4.5 of the Community Land Model (CLM), NCAR Technical Note NCAR/TN-503+STR* (434 pp.). Boulder, CO: National Center for Atmospheric Research.

Peng, X., Frauenfeld, O. W., Cao, B., Wang, K., Wang, H., Su, H., et al. (2016). Response of changes in seasonal soil freeze/thaw state to climate change from 1950 to 2010 across china. *Journal of Geophysical Research: Earth Surface*, *121*, 1984–2000. https://doi.org/10.1002/2016JF003876

Picard, G., Quegan, S., Delbart, N., Lomas, M. R., Toan, T. L., & Woodward, F. I. (2005). Bud-burst modeling in Siberia and its impact on quantifying the carbon budget. *Global Change Biology*, *11*(12), 2164–2176. https://doi.org/10.1111/j.1365-2486.2005.01055.x

Qin, J., Yang, K., Liang, S., & Guo, X. (2009). The altitudinal dependence of recent rapid warming over the Tibetan Plateau. *Climatic Change*, *97*(1-2), 321–327. https://doi.org/10.1007/s10584-009-9733-9

Qin, D. H., Zhou, B. T., & Xiao, C. D. (2014). Progress in studies of cryospheric changes and their impacts on climate of China. *Journal of Meteorology Research*, *28*(5), 732–746. https://doi.org/10.1007/s13351-014-4029-z

Randerson, J. T., Field, C. B., Fung, I. Y., & Tans, P. P. (1999). Increases in early season ecosystem uptake explain recent changes in the seasonal cycle of atmospheric CO_2 at high northern latitudes. *Geophysical Research Letters*, *26*(17), 2765–2768. https://doi.org/10.1029/1999GL900500

Rawlins, M. A., McDonlad, K. C., Frolking, S., Lammers, R. B., Fahnestock, M., Kimball, J. S., & Vorosmarty, C. J. (2005). Remote sensing of snow thaw at the pan-Arctic scale using the SeaWinds scatterometer. *Journal of Hydrology*, *312*(1-4), 294–311. https://doi.org/10.1016/j.jhydrol.2004.12.018

Rawlins, M. A., Nicolsky, D. J., McDonald, K. C., & Romanovsky, V. E. (2013). Simulating soil freeze/thaw dynamics with an improved pan-Arctic water balance model. *Journal of Advances in Modeling Earth Systems*, *5*(4), 659–675. https://doi.org/10.1002/jame.20045

Rienecker, M. M., Suarez, M. J., Gelaro, R., Todling, R., Bacmeister, J., Liu, E., et al. (2011). MERRA: NASA's Modern-Era Retrospective Analysis for Research and Applications. *Journal of Climate*, *24*(14), 3624–3648. https://doi.org/10.1175/JCLI-D-11-00015.1

Saha, S., Moorthi, S., Pan, H. L., Wu, X., Wang, J., Nadiga, S., et al. (2010). The NCEP Climate Forecast System Reanalysis. *Bulletin of the American Meteorological Society*, *91*(8), 1015–1058. https://doi.org/10.1175/2010BAMS3001.1

Schaefer, K., Zhang, T., Slater, A. G., Lu, L., Etringer, A., & Baker, I. (2009). Improving simulated soil temperatures and soil freeze/thaw at high-latitude regions in the Simple Biosphere/Carnegie-Ames-Stanford Approach model. *Journal of Geophysical Research*, *114*, F02021. https://doi.org/10.1029/2008JF001125

Schwartz, M. D., Ahas, R., & Aasa, A. (2006). Onset of spring starting earlier across the Northern Hemisphere. *Global Change Biology*, *12*(2), 343–351. https://doi.org/10.1111/j.1365-2486.2005.01097.x

Shi, X., Mao, J., Thornton, P. E., & Huang, M. (2013). Spatiotemporal patterns of evapotranspiration in response to multiple environmental factors simulated by the Community Land Model. *Environmental Research Letters*, *8*(2), 024012. https://doi.org/10.1088/1748-9326/8/2/024012

Sinha, T., & Cherkauer, K. A. (2008). Time series analysis of soil freeze and thaw processes in Indiana. *Journal of Hydrometeorology*, *9*(5), 936–950. https://doi.org/10.1175/2008JHM934.1

Slater, A. G., Pitman, A. J., & Desborough, C. E. (1998). Simulation of freeze-thaw cycles in a general circulation model land surface scheme. *Journal of Geophysical Research*, *103*(D10), 11,303–11,312. https://doi.org/10.1029/97JD03630

Smith, N. V., Saatchi, S. S., & Randerson, J. T. (2004). Trends in high northern latitude soil freeze and thaw cycles from 1988 to 2002. *Journal of Geophysical Research*, *109*, D12101. https://doi.org/10.1029/2003JD004472

Sun, B. (2017). Seasonal evolution of the dominant modes of the Eurasian snowpack and atmospheric circulation from autumn to the subsequent spring and the associated surface heat budget. *Atmospheric and Oceanic Science Letters*, *10*(3), 191–197. https://doi.org/10.1080/16742834.2017.1286226

Swenson, S. C., Lawrence, D. M., & Lee, H. (2012). Improved simulation of the terrestrial hydrological cycle in permafrost regions by the Community Land Model. *Journal of Advances in Modeling Earth Systems*, *4*(3), M08002. https://doi.org/10.1029/2012MS000165

Thornton, P. E., Doney, S. C., Lindsay, K., Moore, J. K., Mahowald, N., Randerson, J. T., et al. (2009). Carbon-nitrogen interactions regulate climate-carbon cycle feedbacks: Results from an atmosphere-ocean general circulation model. *Biogeosciences*, *6*(10), 2099–2120. https://doi.org/10.5194/bg-6-2099-2009

Toure, A., Rodell, M., Yang, Z., Beaudoing, H., Kim, E., Zhang, Y., & Kwon, Y. (2016). Evaluation of the snow simulations from the Community Land Model, version 4 (CLM4). *Journal of Hydrometeorology*, *17*(1), 153–170. https://doi.org/10.1175/JHM-D-14-0165.1

Viovy, N. (2011). CRUNCEP dataset Retrieved from http://www.cesm.ucar.edu/models/cesm1.2/clm/clm_forcingdata_esg.html

Wang, A. H., & Zeng, X. B. (2009). Improving the treatment of the vertical snow burial fraction over short vegetation in the NCAR CLM3. *Advances in Atmospheric Sciences*, *26*(5), 877–886. https://doi.org/10.1007/s00376-009-8098-3

Wang, C., Dong, W., & Wei, Z. (2003). Study on relationship between the frozen-thaw process in Qinghai-Xizang Plateau and circulation in East-Asia. *Chinese Journal of Geophysics*, *46*, 310–312.

Wang, G., Hu, H., & Li, T. (2009). The influence of freeze–thaw cycles of active soil layer on surface runoff in a permafrost watershed. *Journal of Hydrology*, *375*(3-4), 438–449. https://doi.org/10.1016/j.jhydrol.2009.06.046

Wang, K., Zhang, T., & Zhong, X. (2015). Changes in the timing and duration of the near-surface soil freeze/thaw status from 1956 to 2006 across China. *The Cryosphere*, *9*(3), 1321–1331. https://doi.org/10.5194/tc-9-1321-2015

Wang, A., Zeng, X., & Guo, D. (2016). Estimates of global surface hydrology and heat fluxes from the Community Land Model (CLM4.5) with four atmospheric forcing datasets. *Journal of Hydrometeorology*, *17*(9), 2493–2510. https://doi.org/10.1175/JHM-D-16-0041.1

Xie, Z. H., Wang, L., Jia, B., & Yuan, X. (2016). Measuring and modeling the impact of a severe drought on terrestrial ecosystem CO_2 and water fluxes in a subtropical forest. *Journal of Geophysical Research: Biogeosciences*, *121*, 2576–2587. https://doi.org/10.1002/2016JG003437

Yang, M. X., Nelson, F., Shiklomanov, N., Guo, D. L., & Wan, G. (2010). Permafrost degradation and its environmental effects on the Tibetan Plateau: A review of recent research. *Earth Science Reviews*, *103*(1-2), 31–44. https://doi.org/10.1016/j.earscirev.2010.07.002

Yang, K., Wu, H., Qin, J., Lin, C., Tang, W., & Chen, Y. (2014). Recent climate changes over the Tibetan Plateau and their impacts on energy and water cycle: A review. *Global and Planetary Change*, *112*, 79–91. https://doi.org/10.1016/j.gloplacha.2013.12.001

Yi, S., Arain, M. A., & Woo, M. K. (2006). Modifications of a land surface scheme for improved simulation of ground freeze-thaw in northern environments. *Geophysical Research Letters*, *33*, L13501. https://doi.org/10.1029/2006GL026340

Yi, S., Zhou, Z., Ren, S., Xu, M., Qin, Y., Chen, S., & Ye, B. (2011). Effects of permafrost degradation on alpine grassland in a semi-arid basin on the Qinghai-Tibetan Plateau. *Environmental Research Letters*, *6*(4), 045403. https://doi.org/10.1088/1748-9326/6/4/045403

Zeng, X., & Decker, M. (2009). Improving the numerical solution of soil moisture–based Richards equation for land models with a deep or shallow water table. *Journal of Hydrometeorology*, *10*(1), 308–319. https://doi.org/10.1175/2008JHM1011.1

Zhang, T. (2005). Influence of the seasonal snow cover on the ground thermal regime: An overview. *Reviews of Geophysics*, *43*, RG4002. https://doi.org/10.1029/2004RG000157

Zhang, T., & Armstrong, R. L. (2001). Soil freeze/thaw cycles over snow-free land detected by passive microwave remote sensing. *Geophysical Research Letters*, *28*(5), 763–766. https://doi.org/10.1029/2000GL011952

Zhang, T., Armstrong, R. L., & Smith, J. (2003). Investigation of the near-surface soil freeze-thaw cycle in the contiguous United States: Algorithm development and validation. *Journal of Geophysical Research*, *108*(D22), 8860. https://doi.org/10.1029/2003JD003530

Zhao, L., Ping, C. L., Yang, D. Q., Cheng, G. D., Ding, Y. J., & Liu, S. Y. (2004). Changes of climate and seasonally frozen ground over the past 30 years in Qinghai–Xizang (Tibetan) Plateau, China. *Global and Planetary Change*, *43*(1-2), 19–31. https://doi.org/10.1016/j.gloplacha.2004.02.003

Zhou, B. T., Xu, Y., Wu, J., Dong, S., & Shi, Y. (2016). Changes in temperature and precipitation extreme indices over China: Analysis of a high-resolution grid dataset. *International Journal of Climatology*, *36*(3), 1051–1066. https://doi.org/10.1002/joc.4400